

## PERFORMANCE OF THE OPAL SI-W LUMINOMETER AT LEP I-II

G. ABBIENDI

*Dipartimento di Fisica dell'Università di Bologna and INFN,  
Viale Berti Pichat 6/2, 40127 Bologna, Italy  
E-mail: Giovanni.Abbiendi@bo.infn.it*

R. G. KELLOGG

*Department of Physics, University of Maryland, College Park, MD 20742, USA  
E-mail: Richard.Kellogg@cern.ch*

D. STROM

*University of Oregon, Department of Physics, Eugene OR 97403, USA  
E-mail: strom@bovine.uoregon.edu*

A pair of compact Silicon-Tungsten calorimeters was operated in the OPAL experiment at LEP to measure the integrated luminosity from detection of Bhabha  $e^\pm$  scattered at small angles from the beam line. The performance of the detector at both LEP-I and LEP-II is reviewed.

### 1. Introduction

The LEP  $e^+e^-$  collider at CERN operated for more than a decade: in 1989-95 at center of mass energies close to the  $Z$  peak (LEP-I); in 1996-2000 at higher energies, up to 209 GeV (LEP-II). In the first phase a large number of  $Z^0$  events were collected, of the order of  $5 \times 10^6$  events per experiment. To match the inherent precision of this data sample, the error on the integrated luminosity had to be better than  $10^{-3}$ . At LEP the relevant process for the luminosity measurement is Bhabha scattering at small angle, which delivers a counting rate higher than the  $Z^0$  event rate at resonance. The Bhabha angular spectrum falls like  $1/\theta^3$ , implying a high sensitivity to the definition of the minimum polar angle of the acceptance. For example an uncertainty  $\delta\theta = 10 \mu\text{rad}$  (which in our configuration is equivalent to  $25 \mu\text{m}$  in radius at the face of the detector) would give an unacceptable systematic error of  $10^{-3}$ . Precision luminosity measurement was thus a demanding task, dictated by interest in measuring absolute cross sections at the  $Z^0$  peak. In particular,

cross sections were needed to determine the Invisible Ratio  $R_{inv} = \Gamma_{inv}/\Gamma_{ll}$ , the ratio of the  $Z$  decay width to invisible particles and to charged lepton pairs. From  $R_{inv}$  the LEP experiments determined the number of light neutrinos to be 3 and limited possible contributions from extra new physics like cold dark matter. <sup>a</sup>

## 2. Detector

The OPAL Si-W luminometer consists of 2 identical cylindrical calorimeters, encircling the beam pipe symmetrically at  $\pm 2.5$  m from the interaction point. A detailed description can be found in the OPAL paper <sup>1</sup>. Each calorimeter is a stack of 19 silicon layers interleaved with 18 tungsten plates, with a sensitive depth of 14 cm, representing  $22 X_0$ . The first 14 tungsten plates are each  $1 X_0$  thick, while the last 4 are each  $2 X_0$  thick. The sensitive area fully covers radii between 6.2 and 14.2 cm from the beam axis, giving a total area of silicon of  $1.0 \text{ m}^2$  per calorimeter. Each silicon layer is divided into 16 overlapping wedges. Even and odd layers are staggered by an azimuthal rotation of half a wedge. Water cooling pipes run as close as possible to the readout chips to remove the 340 W dissipated in each calorimeter. The distribution of material upstream of the calorimeters is kept at a minimum especially in the crucial region of the inner acceptance cut where it amounts to  $0.25 X_0$ . In the middle of the acceptance this material increases to about  $2 X_0$  due to cables and support structures of the beam pipe. The effects of the degraded energy resolution are important and are corrected for.

Each detector wedge is a thick-film ceramic hybrid carrying a 64-pad silicon wafer diode plus the readout electronics. The pad layout of the silicon diodes is shown in Figure 1. The pads are arranged in a  $R - \phi$  geometry, with a radial pitch of 2.5 mm. Readout is done with 4 DC-coupled AMPLEX chips (each one reading 16 channels in a given  $\phi$  column). The diodes have an average depletion voltage of 62 V and are operated at 80 V bias voltage. The complete luminometer has in total 608 wedges with a total of 38,912 readout channels.

For a typical LEP-I Bhabha electron with  $E_e = 45$  GeV the charge deposited on a single detector layer at shower maximum is 300 – 400 mips ( $\approx 1.0 - 1.3$  pC) which is typically spread over a few pads. The AMPLEX chip has a full scale limit of more than 1000 mips for each pad, thus providing a sufficient dynamic range. The equivalent noise for each channel remained at a level of 1500 to 2000 electrons for a typical detector capacitance of 20 pF, giving better than 10 : 1 signal to noise for mips.

---

<sup>a</sup>OPAL results are  $N_\nu = 2.984 \pm 0.013$  and  $\Gamma_{inv}^{new} < 3.7$  MeV at 95% confidence level.

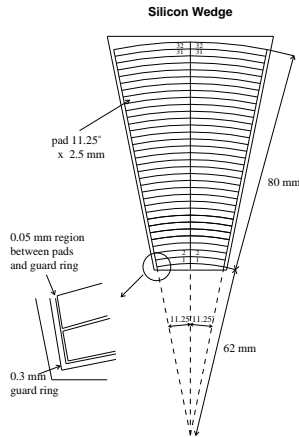


Figure 1. Layout of the pad geometry of one wedge.

The calibration has been studied with electrical pulses generated both on the AMPLEX chips themselves and on the hybrids, as well as with ionization signals generated in the Si using test beams and laboratory sources. The overall channel-to-channel uniformity in gain was 1 % but gain variations among the 16 channels of each AMPLEX were  $\leq 0.25\%$ . This allowed optimum resolution for trigger thresholds and eliminated the need for a database of calibration constants for off-line energy reconstruction. Cross talk among channels in each AMPLEX was at the level of 2%/channel (coherent 30 %/AMPLEX) and was subtracted. Any residual gain variations depending on the channel position within each AMPLEX were cancelled by inverting the channel radial ordering between the two  $\phi$  columns of each wedge.

The calorimeters were exposed to substantial radiation from occasional catastrophic beam losses. To limit this damage a protection system monitored the bias currents and induced a fast beam dump if the absorbed energy was greater than  $3 \times 10^8$  GeV within 1 s. The leakage current at 22°C was uniformly 1 nA/cm<sup>2</sup> when the detector was installed in 1993. Radiation damage during eight years of operation at LEP increased it to 12 nA/cm<sup>2</sup> on average, although at shower maximum the typical values are 5 times higher (the AMPLEX bias current limit is  $\approx 200$  nA/pad). From such increase of the leakage current we have estimated an effective absorbed dose of about 4 Krad, or a total absorbed energy of  $\approx 5 \times 10^{12}$  GeV, using measurements from J. Lauber et al. <sup>2</sup>. At the end of LEP running only 0.6% of the Si-W Luminometer was not functional.

### 3. Lateral shower profile

The lateral profile of electromagnetic showers in the dense medium of the Si-W calorimeters is characterized by a sharp central peak (FWHM  $< 1$  pad = 2.5 mm) and broad tails extending to almost 10 pads, as shown in Fig. 2.

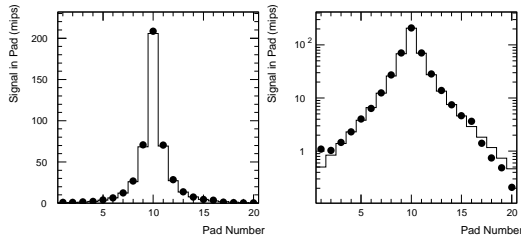


Figure 2. Average radial shower profile at  $6 X_0$  for  $E = 45.5$  GeV electrons in linear (*left*) and logarithmic (*right*) scale.

Peak finding is based on the second spatial derivative of the pad charge, so that a sufficiently pronounced shoulder can be identified as a secondary cluster. Radiative Bhabha events with one or more photons contained within the acceptance can produce such configurations. The two cluster resolution efficiency has been determined from such radiative data events with a well separated secondary cluster with  $E > 5$  GeV. The pad signals belonging to the secondary cluster are rotated about the beam axis until they have the same azimuth as the primary cluster and added to the signals actually observed on the local pads. The standard reconstruction is then applied and the separation efficiency as a function of the radial distance between the two clusters is obtained, as shown in Fig. 3. It is greater than 50% for cluster separation greater than 1.0 cm, equivalent to 4 pad widths. The overall inefficiency of primary cluster finding is less than  $10^{-5}$ .

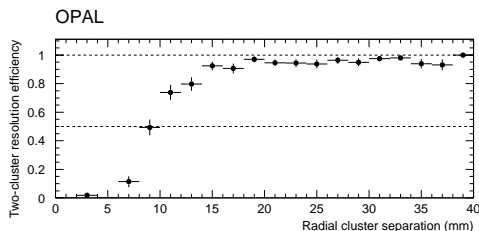


Figure 3. Efficiency of reconstructing a secondary cluster as a function of the radial separation with the primary one when they have equal azimuth.

#### 4. Position measurement

The detector segmentation is very different in  $R$  and  $\phi$ , owing to their different impact on the luminosity measurement. Here we will be interested only in the precise radial position measurement.

The radial coordinate is first determined in each layer by interpolating a coordinate within the pad displaying the maximum signal in that layer. Then all the good layer coordinates from  $2 X_0$  to  $10 X_0$  in depth are projected onto a reference layer chosen at  $7 X_0$ , and averaged there. The reference layer lies near the average shower maximum to minimize systematic effects. The resolution of the layer coordinate varies strongly across a pad, from about  $300 \mu\text{m}$  at pad boundaries to  $750 \mu\text{m}$  at pad center. This variation is reflected even in the average  $R$  coordinate, where a periodical structure following the radial pitch is apparent. To remove such oscillation, as the last step, a smoothing algorithm is applied, subjected to boundary conditions at the pad boundaries.

A key issue for the luminosity measurement is knowledge of the absolute radial dimensions of the calorimeters. Very accurate positioning and monitoring of detector wedges in each layer using microscopes and micro-manipulators have achieved an RMS scatter of  $1.3 \mu\text{m}$  of the radius of each wedge with respect to the best-fit circle of each half-layer. Taking into account deviations of each half-layer with respect to its ideal position in the calorimeter stack, mechanical deformations, temperature effects and measurement errors, the final precision on the absolute average radius is  $4.4 \mu\text{m}$ .

The final position resolution of the average smoothed radial coordinate has been determined to be  $130 \mu\text{m}$  at pad boundaries and  $170 \mu\text{m}$  at pad centers, from test beam measurements. The test beam used a 45 GeV electron beam alternated with a 100 GeV muon beam. Alignment of the calorimeter with respect to a high resolution Si-strip beam telescope was carried out with the muon beam. Sensitivity of the Si-W electronics to mips was essential for this purpose. The effect of upstream material was studied using a  $0.84 X_0$  plate which could be inserted in front of the detector.

The reconstruction method respects the symmetry condition that a shower which deposits equal energies on two adjacent pads in the reference layer at  $7 X_0$  has to be reconstructed in the mean exactly at the boundary between the pads. In reality due to the  $R - \phi$  geometry of the pads, the true position of such showers is at a smaller radius than the pad boundary. This is the so called *pad boundary bias*, which depends on the lateral shower spread and has been measured in the test beam. As the radial position of the incoming particles is scanned across a radial pad boundary in a single layer, the probability for observing the largest pad signal above or below this boundary

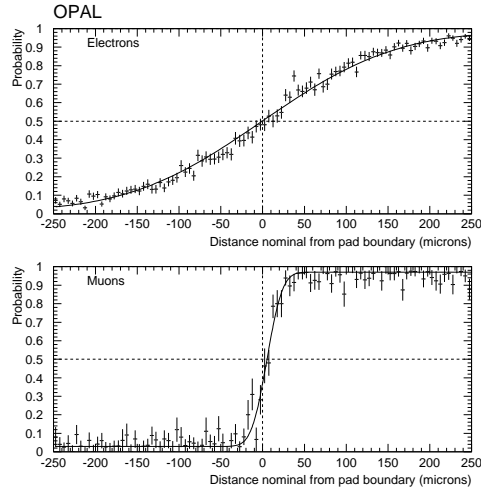


Figure 4. Pad boundary images for test beam electrons and muons at  $7 X_0$ .

shifts rapidly, giving an image of the pad boundary as shown in Fig 4. The pad boundary images are modelled with an error function, where the gaussian width  $w$  is called the pad boundary transition width and  $R_{off}$  is the radial offset between the apparent and the nominal pad boundary. The difference in  $R_{off}$  obtained by changing from electron to muon beam is the measured pad boundary bias, which is shown in Fig. 5 as a function of  $w$ . The reconstructed radial coordinate is sensitive to the distribution and type of material in front of the detector as well as to the incidence angle of the particles. The test beam configuration could not reproduce the exact features of the OPAL running, so an indirect approach has been followed, called *anchoring*. Details of the method are fully explained in the cited paper <sup>1</sup>. The procedure is applied separately on individual data samples, each one characterized by different beam parameters, and obtains net systematic corrections on the radius of the acceptance cuts. The inner acceptance cut is corrected by 5-10  $\mu\text{m}$  with an uncertainty of 3.5  $\mu\text{m}$ , while the outer acceptance cut is corrected by 10-20  $\mu\text{m}$  with an uncertainty of 6  $\mu\text{m}$ . These radial corrections are then easily turned into acceptance corrections which are applied to data.

We have also studied the energy dependence of the pad boundary transition width using data from OPAL running, as there was no test beam data at LEP-II energies. In Fig. 6  $w$  is plotted as a function of depth into the calorimeter for LEP-I and LEP-II Bhabha electrons. There is a sizeable shrinkage of the shower core with increasing energy. As  $w$  is related to the position resolution

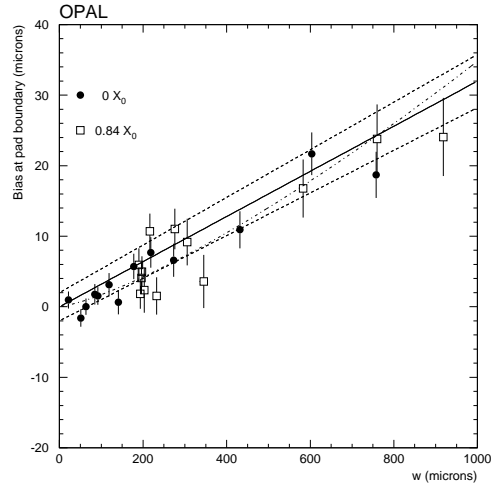


Figure 5. The pad boundary bias as a function of the pad boundary transition width  $w$ . The points refer to different depths in the bare calorimeter (solid circles) or after an optional preshowering layer (open boxes).

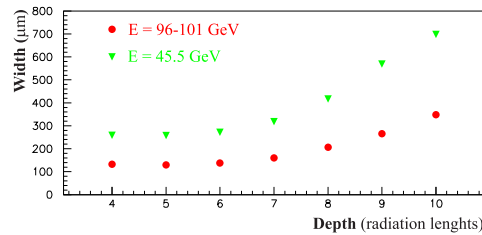


Figure 6. Pad boundary transition width as a function of depth in the calorimeter at a fixed radius for LEP-I and LEP-II energies.

near the pad boundaries, this indicates that the radial resolution inherently improves at energies higher than LEP-I.

## 5. Energy measurement

The distribution of the summed energy in the left and right calorimeters (after all other cuts) is shown in Fig. 7 for a typical OPAL run. The bulk of selected Bhabha events have back-to-back electrons and positrons with energies close to the beam energy. The large accidental background is visible at small en-

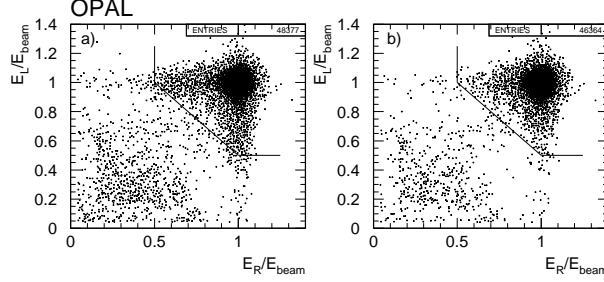


Figure 7. Distribution of  $E_L$  vs  $E_R$  after all selection cuts except for the energy cuts and before the acollinearity cut (a) or after it (b). The lines show the cuts applied to the energies.

ergies and is reduced to negligible levels by applying tight energy cuts, which also eliminate a small fraction of real Bhabha events. The visible radiative tails extending from the full energy spot originate from events which have lost energy due to a single initial state photon emitted along the beam axis. For these events transverse momentum conservation implies:  $E_R/E_L = R_L/R_R$ . A useful quantity to improve our understanding of the Bhabha events failing the energy cut is the radius difference or acollinearity  $\Delta R = R_R - R_L$ . A cut at  $\Delta R < 10$  mrad reduces both the background and the impact of uncertainties in the low energy tail of the detector response function, as can be seen from Fig. 7/a-b. The systematic error due to the energy measurement is reduced by almost a factor 3 with the  $\Delta R$  cut. By cutting on the acollinearity one can also effectively limit or constrain the energy lost to initial state radiation. Therefore it is also useful to provide clean samples of beam energy electrons for studying the energy response of the calorimeters. Also samples with a selected lower energy can be isolated, though with lower statistics. The energy resolution has stayed almost constant during all the LEP running. At LEP-I ( $E \approx 45$  GeV)  $\Delta E/E = 3.8 - 4.5\%$  (for right - left calorimeter); at LEP-II ( $E \leq 104$  GeV)  $\Delta E/E = 5.0\%$  (for both right and left calorimeter). Differences between the two calorimeters as well as from LEP-I and LEP-II are due to different amounts of preshowering material.

## 6. Final error on luminosity

The main experimental systematic errors on the OPAL luminosity measurement at LEP-I<sup>1</sup> are summarized in table 1. After all the effort on radial reconstruction, the dominant systematic error is related to the energy measurement, mostly due to uncertainties in the tail of the energy response function and the

Table 1. The most important systematic errors in the final luminosity measurement for LEP-I.

Systematic errors	$\times 10^{-4}$
Energy	1.8
Inner Anchor	1.4
Radial Metrology	1.4
Total Experimental	3.4
Total Theoretical	5.4

nonlinearity. The final experimental systematic error successfully matches the desired level of precision, well below  $10^{-3}$ , and even surpasses the present theoretical precision of the calculated Bhabha cross section, which is one of the most deeply studied QED processes.

## 7. Conclusions

The OPAL Si-W luminometer has reliably operated at LEP for 8 years (1993-2000), with high efficiency and negligible losses of Si detectors and readout electronics in a non-trivial background environment. Its performance can be summarized by these figures:

- (1) Energy resolution  $\approx 4\%$  almost constant from  $E = 45$  GeV to  $E = 100$  GeV;
- (2) Good efficiency to resolve close lying clusters:  $\epsilon \geq 50\%$  for  $\Delta R \geq 1.0$  cm;
- (3) Good S/N ratio for mips: 10/1;
- (4) Position resolution on the radial coordinate of 130-170  $\mu\text{m}$  with a residual bias less than 7  $\mu\text{m}$ .

In particular the very small residual bias on the position of the acceptance cut was crucial to achieve the extraordinary experimental systematic error of only  $3.4 \times 10^{-4}$ .

## References

1. OPAL Collaboration, G. Abbiendi et al., *Eur. Phys. J.* **C14**, 373 (2000).
2. J. A. Lauber, S. Gascon-Shotkin, R. G. Kellogg, G. R. Martinez, *Nucl. Instrum. Meth.* **A396**, 165 (1997).